Figure 2 compares typical temperature and pressure-drop histories from Ref. 4 with those predicted by the models. Again, the nonequilibrium model gives significantly improved predictions. Figure 3 compares axial T_w distributions at two different cooldown times with similar results. Steady-state boiling heat-transfer data[3] provides another independent check on the analytical model. Predicted wall temperature distributions for three tests (Fig. 4) are low, but the general trends and the magnitudes are in good agreement. This suggests that the inlet conditions assumed are probably in error (following Hendricks, it was assumed that the inlet fluid was 100% liquid). Axial heat conduction upstream probably caused some prevaporization of liquid. The higher actual vapor qualities should lead to lower effective heat-transfer coefficients and thus higher wall temperatures.

Discussions

It was recognized that the correct measurement of the bulk fluid temperature depends on the slug frequency (in mist and slug flows) and on the thermocouple and galvanometer response times. An analysis showed that the maximum thermocouple and galvanometer response times for the conditions studied is approximately 5 msec; hence slug flow with slug frequencies as high as 100 may be detected.

For the chilldown of the Cu test section, the maximum slug frequency observed was $\sim$30. In general, the frequency was on the order of 2.5 or less. The liquid slug residence times increased with chilldown; the minimum occurring at the initiation of chilldown was on the order of 10–20 sec. Vapor slug residence times, on the other hand, remained at a high level throughout film boiling. Under these conditions, liquid slugs can be readily detected; and true separated-phase temperatures in the film-boiling regime can be measured with negligible errors. The transient test approach used in this study permitted the determination of local heat-transfer data over a wide range of conditions with a minimum number of tests.

For the development of a general equation to predict forced convection film boiling, it was postulated that slug flow occurs with discrete slugs of vapor and liquid. Although the experimental data included transitions from single phase to mist flow and then to slug flow, the generally good agreement between observed and predicted transient and steady-state properties suggest that the idealized slug flow model is satisfactory for the general determination of forced convective film boiling heat flux and for heat-transfer calculations.

References

[1] Core, T. C., Harkee, J. F., Misra, A., and Sato, K., "Heat Transfer Studies," WADD-60-239, 1959, Wright Air Development Div., Wright-Patterson Air Force Base, Ohio.

[2] Wright, C. C. and Walters, H. H., "Single Tube Heat Transfer Tests—Gaseous and Liquid Hydrogen," WADC-TR-59-423, 1959, Wright Air Development Center, Wright-Patterson Air Force Base, Ohio.

[3] Hendricks, R. C., Graham, R. W., Hsu, Y. Y., and Friedman, R., "Experimental Heat Transfer and Pressure Drop of Liquid Hydrogen Flowing Through a Heated Tube," TN-D-765, 1961, NASA.

[4] Chenoweth, F., Watt, J. J., and Sprague, E. L., "Transient Chilldown of a Single Thick-Walled Tube by Liquid and Gaseous Hydrogen," TND-4238, 1967, NASA.

[5] Chi, J. W. H. and Vetere, A. M., "Two-Phase Flow During Transient Boiling of Hydrogen and Determination of Non-Equilibrium Vapor Fractions," *Advances in Cryogenic Engineering*, Vol. 9, Plenum Press, New York, 1964.

[6] Chi, J. W. H., "Effect of Mist Flow on Cool-Down Temperatures and Cool-Down Time," *Advances in Cryogenic Engineering*, Vol. 10, Plenum Press, New York, 1965.

[7] Chi, J. W. H., "A Correlation for Forced Convection Heat Transfer to Hydrogen," *Journal of Spacecraft and Rockets*, Vol. 3, No. 1, Jan. 1966, pp. 150–152.

[8] Chi, J. W. H., "Slug Flow and Film Boiling of Hydrogen," *Journal of Spacecraft and Rockets*, Vol. 4, No. 10, Oct. 1967, pp. 1329–1332.

Time-Dependent Solutions of Nonequilibrium Dissociating Flow past a Blunt Body

C. P. Li*

Lockheed Electronics Company Inc., Houston, Texas

Introduction

ANALYSIS of the chemical nonequilibrium flow past a blunt body at hypersonic speed has received much attention in recent years. A number of numerical techniques have been developed and applied to this problem with considerable success. It appears, however, that some of the techniques are inherently restricted to a two-dimensional flowfield calculation due to the algebraic complexities involved or the prohibitive computing time consumed when flow asymmetries are considered.[1,2] The coupling of chemical kinetic equations with the fluid-dynamic equations apparently tends to worsen the numerical difficulty already existing in these techniques. This Note describes an alternative technique that is simple and fast compared to others and can be applied to calculate nonequilibrium blunt body flows at high angles of attack.

The time-dependent technique used in this study is based largely on the work of Moretti and others[3] on a three-dimensional ideal gas blunt body flow problem. The bow shock is treated as a moving discontinuous surface and the computation of the flowfield is confined within a region bounded by the shock and body. A set of unsteady governing equations in nonconservative form is chosen and its asymptotic solution is considered to be the steady-state flowfield solution being sought. The continuous shock layer region is calculated by a second-order explicit finite-difference method, and boundary conditions at the shock and body are implemented using a quasi-one-dimensional, unsteady method of characteristics. The straightforward extension of Ref. 3 to account for the coupled dissociation-recombination processes is made by using three different equations: 1) an equation with pressure as the dependent variable, 2) an energy equation to replace the entropy equation, and 3) a chemical kinetic equation. For ease of computation and comparison with published data, an ideal dissociating diatomic gas model was selected for this paper. Numerical results discussed here include an oxygen gas flow past a sphere and a nitrogen gas flow past an ellipsoid at a 20° angle of attack. The results for oxygen flow past a sphere are compared with results obtained from a method of integral relations.[2]

Received December 9, 1970; revision received March 25, 1971. This work was supported by the Manned Spacecraft Center under NASA Contract 9-5384. The author gratefully acknowledges the help given by W. Reicks.

* Staff Engineer, Aeromechanics Section, Houston Aerospace Systems Division. Member AIAA.

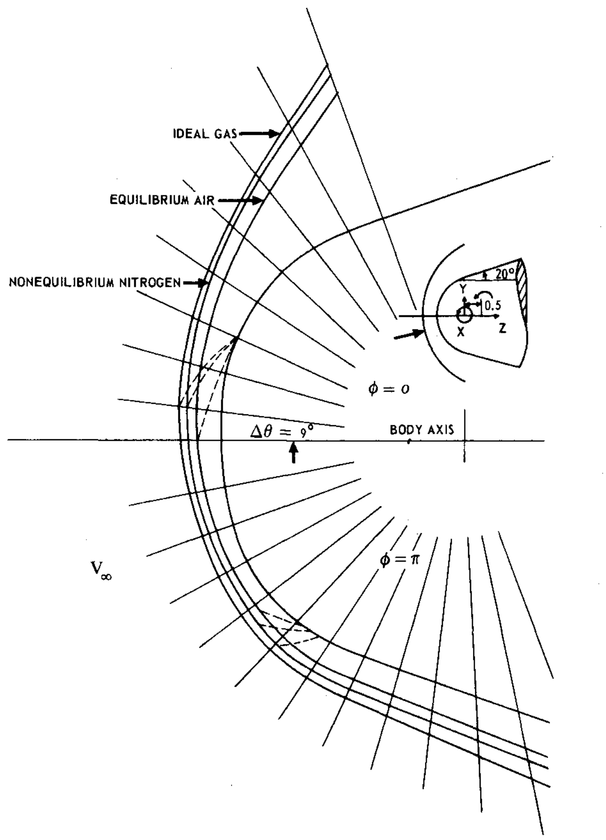

Fig. 1 Shock wave and sonic line shapes for a nonequilibrium nitrogen flow on the symmetry plane of an ellipsoid at a 20° angle of attack.

Governing Equations

The set of equations governing the flow of an ideal dissociating gas in chemical nonequilibrium are

$$\frac{dp}{dt} + \frac{4+\alpha}{3} p \operatorname{div}\mathbf{u} + \left(\frac{p}{1+\alpha} - \frac{(1+\alpha)\rho\theta_d}{3}\right)\omega = 0 \quad (1)$$

$$d\mathbf{u}/dt + \operatorname{grad}p/\rho = 0 \quad (2)$$

$$de/dt + p \operatorname{div}\mathbf{u}/\rho = 0 \quad (3)$$

$$d\alpha/dt + \omega = 0 \quad (4)$$

$$p = (1+\alpha)R\rho T \quad (5)$$

$$e = [3/(1+\alpha)]p/\rho + \alpha\theta_d \quad (6)$$

where $d/dt = \partial/\partial t + \mathbf{u}\cdot\text{grad}$, and the vector operators are to be defined in a spherical polar coordinate system (r,θ,ϕ). The rate of change of the mass fraction ω is obtained from

$$\omega = -CT^\eta\rho[(1-\alpha)\exp(-\theta_d/T) - \alpha^2\rho/\rho_d] \quad (7)$$

The quantities p,ρ,T,e,α, and $\mathbf{u}$ are, respectively, the pressure,

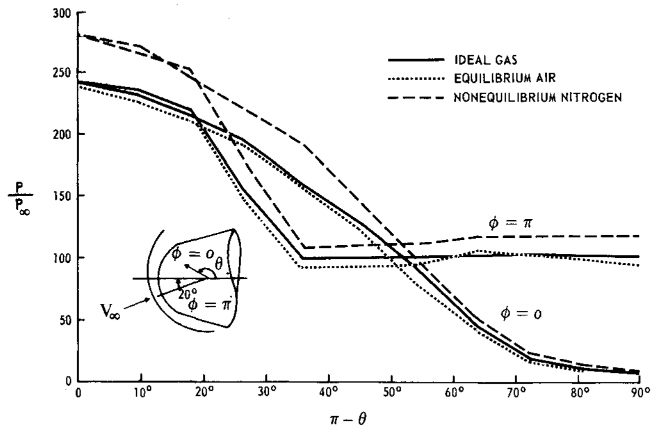

Fig. 2 Nonequilibrium nitrogen pressure distribution on the symmetry plane.

density, temperature, specific internal energy, degree of dissociation, and velocity. The gas constant of the diatomic species is represented by R. Parameters in Eq. (7) are determined from a procedure suggested by Capiaux and Washington.[4] The rate constants for N_2 and O_2 were obtained, respectively, from Matthews[5] and Hammerling and others.[6] A list of these parameters can be found in Ref. 7.

Method of Solution

As discussed in Ref. 3, the shock layer region is transformed into a parallelepiped and then divided into a number of even-spaced meshes. The Taylor series expansion truncated after the third term is used to advance the solution in a time-iterative procedure. The steady-state solution is reached when the differences in flow quantities calculated at two consecutive time steps become negligible. The number of time steps needed to accomplish a steady-state solution is principally dependent upon the closeness of the assumed initial flow distributions to the final solution. For example, when the degree of dissociation α is set equal to zero in the shock layer region at the beginning of the calculation $t = 0$ the computing time is longer than if a more realistic α were chosen.

The time increment between two successive time steps is determined from two criteria. One is obtained from the Courant-Friedrichs-Lewy (CFL) analysis, requiring that the time increment $\tau_1 \leq \Delta s/1.5(a_f + q)$, where Δs represents the minimum mesh size, a_f the frozen sonic speed, and q the flow speed. The other criterion for obtaining a useful time increment originates from the chemical reaction relaxation time; it requires $\tau_2 \leq 0.1/|\omega|$, where ω is given in Eq. (7). The use of τ_2 in the Taylor expansion insures that no numerical instability will occur due to the stiffness of the rate Eq. (4). The justification of using τ_2 is based on an argument similar to that used for τ_1 in which τ_1 is made equal to or less than the physical time necessary for a disturbance to propagate the distance of one mesh space. Anderson[8] has

Table 1 Nonequilibrium oxygen flow properties on a sphere[a]

θ, deg	Shock standoff distance		p/p_∞		T/T_∞		$v/(p_\infty/\rho_\infty)^{1/2}$		α	
	Ref. 2[b]	Present[c]	Ref. 2[b]	Present[c]	Ref. 2[b]	Present[c]	Ref. 2[b]	Present[c]	Ref. 2[b]	Present[c]
0.00	0.0907	0.0861	133.09	130.0	11.28	11.6	0.00	0.00	0.114	0.176
7.162	0.0917	0.0875	130.58	127.3	11.21	11.5	0.693	0.815	0.114	0.175
14.324	0.0949	0.0917	123.35	119.4	11.10	11.5	1.37	1.61	0.114	0.172
21.286	0.100	0.0988	111.93	107.6	10.88	11.4	2.06	2.42	0.113	0.171
28.648	0.109	0.109	97.533	93.58	10.57	11.1	2.76	3.27	0.113	0.164
35.810	0.121	0.122	82.335	77.88	10.18	10.9	3.39	3.99	0.112	0.165
42.972	0.139	0.139	67.284	61.14	9.73	10.6	4.00	4.85	0.112	0.158

[a] $M_\infty = 10$, $p_\infty = 21.17$ lb/ft², $T_\infty = 523°$ R, $\rho_\infty = 2.62 \times 10^{-5}$ slug/ft³.
[b] Integral method (p. 131 of Ref. 2). Scheme I, $N = 2$.
[c] Time-dependent method.

used a similar condition to determine the time increment in a study of time-dependent, nonequilibrium nozzle flows.

The mesh points at the shock and body are computed by a quasi-one-dimensional method of characteristics technique. Equation (1) is written in an intrinsic coordinate system attached to the boundary. Flow variables and their derivatives in the directions other than the normal to the boundary are considered to be forcing functions. The resulting compatibility equation is then integrated along the characteristic lines.

Results and Discussion

The mesh system used in the sphere flowfield calculation consists of five mesh spaces in the radial direction and fifteen mesh spaces in the angular direction. The origin of the coordinate system was located at the center of the sphere. The calculation was terminated after 300 time steps, which consumed 4 min on the UNIVAC 1108. The results for both the time-dependent technique and the method of integral relations as obtained from Ref. 2 are listed in Table 1. The tabulated results indicate that flow quantities other than α and v are in fair agreement. The differences in α and v may be attributed to differences in the gas model and rate constant used in the two analyses. In this calculation τ_2 was about an order of magnitude less than τ_1 and no instabilities occurred in regions of near equilibrium.

The second case is an ellipsoid that has an axis ratio of 1.5 and an afterbody of a 20° half-angle cone. The computational mesh was constructed using seven spacings in the radial direction, 10 in the angular direction, and eight in the azimuthal direction. Figure 1 shows shock and sonic line shapes on the plane of symmetry. The shock configuration predicted by the nonequilibrium calculation is seen to lie between the shocks predicted by the same techniques using ideal gas and equilibrium air models. As shown, the sonic lines are located on the body surface at nearly the same position. A large computation region was used to provide the information necessary for restarting the calculation in the supersonic region using the method of characteristics. The pressure distributions on the body are presented in Fig. 2. The nonequilibrium calculation indicates a slightly higher pressure than that of the other two gas models. Eight hundred time steps were used for the nonequilibrium solution.

The complete solution required approximately 85 min on the UNIVAC 1108. The equilibrium air calculation was obtained with 400 time steps and 57 min of computer time. The ideal gas calculation used 300 time steps and 26 min of computer time. All results were obtained for the same number of mesh points, and the changes of flow variables at the last two successive time steps were indiscernible. The freestream conditions used in this case were $V_\infty = 12{,}500$ fps, $p_\infty = 3.06$ lb/ft^2 and $\rho_\infty = 3.56 \times 10^{-5}$ slug/ft^3.

Conclusion

The nonequilibrium dissociating gas flow has been analyzed using a time-dependent technique for the shock layer around a blunt body at an angle of attack. It has been found that the time increment necessary for obtaining a stable solution must be small enough to satisfy both the CFL criterion and a chemical relaxation time criterion. The results predicted by the time-dependent technique were in reasonable agreement with those of a method of integral relations. It should be noted that the binary scaling principle $\rho_\infty L$ = const is satisfied because the governing Eqs. (1–7) are written in a nondimensional form and because of the dissociation-dominated nature of the chemical reaction. Therefore, the flowfields at different altitudes and for bodies of different characteristic length can be related to the flowfield obtained at a given altitude and body characteristic length.

References

[1] Bohachevsky, I. O. and Rubin, E. L., "A Direct Method for Computation of Nonequilibrium Flows with Detached Shock Waves," *AIAA Journal*, Vol. 4, No. 4, April 1966, pp. 600–607.

[2] Belotserkovskiy, O. M., "Supersonic Gas Flow Around Blunt Bodies," TT F-453, June 1969, NASA.

[3] Moretti, G., Bleich, B., Abbett, M., and Fort, R., "Three-Dimensional Inviscid Flow About Supersonic Blunt Cones at Angle-of-Attack," Vols. 1, 2, and 3, SC-CR-68-3728, Sept. 1968, Sandia Labs., Albuquerque, N.Mex.

[4] Capiaux, R. and Washington, M., "Nonequilibrium Flow Past a Wedge," *AIAA Journal*, Vol. 1, No. 3, March 1963, pp. 650–660.

[5] Matthews, D. L., "Interferometer Measurement in the Shock Tube of the Dissociation Rate of Oxygen," *The Physics of Fluids*, Vol. 2, No. 2, March–April 1959, pp. 170–178.

[6] Hammerling, P., Teare, J. D., and Kivel, B., "Theory of Radiation from Luminous Shock Waves in Nitrogen," *The Physics of Fluids*, Vol. 2, No. 4, July–Aug. 1959, pp. 422–426.

[7] Li, C. P., "Time-Dependent Solutions of Nonequilibrium Binary Mixture Flow Past a Blunt Body," 675-44-31, Sept. 1970, Houston Aerospace Systems Div., Lockheed Electronics Co., Houston, Texas.

[8] Anderson, J. D., "A Time-Dependent Analysis for Vibrational and Chemical Nonequilibrium Nozzle Flows," *AIAA Journal*, Vol. 8, No. 3, March 1970, pp. 545–550.